Marine Geology 369 (2015) 116–126

Contents lists available at ScienceDirect

Marine Geology

journal homepage: www.elsevier.com/locate/margeo

Continental shelf morphology and stratigraphy offshore San Onofre, California: The interplay between rates of eustatic change and sediment supply

Shannon Klotsko [a,*], Neal Driscoll [a], Graham Kent [b], Daniel Brothers [c]

[a] Scripps Institution of Oceanography, UC San Diego, 9500 Gilman Drive, La Jolla, CA 92093, United States
[b] Nevada Seismological Laboratory, University of Nevada, Reno, Laxalt Mineral Engineering Building, Room 322, Reno, NV 89557, United States
[c] U.S. Geological Survey, 400 Natural Bridges Drive, Santa Cruz, CA 95060, United States

ARTICLE INFO

Article history:
Received 31 January 2015
Received in revised form 18 July 2015
Accepted 1 August 2015
Available online 5 August 2015

Keywords:
San Onofre
Continental margin processes
Cristianitos Fault
CHIRP seismic
Transgressive deposits
Sediment controls

ABSTRACT

New high-resolution CHIRP seismic data acquired offshore San Onofre, southern California reveal that shelf sediment distribution and thickness are primarily controlled by eustatic sea level rise and sediment supply. Throughout the majority of the study region, a prominent abrasion platform and associated shoreline cutoff are observed in the subsurface from ~72 to 53 m below present sea level. These erosional features appear to have formed between Melt Water Pulse 1A and Melt Water Pulse 1B, when the rate of sea-level rise was lower. There are three distinct sedimentary units mapped above a regional angular unconformity interpreted to be the Holocene transgressive surface in the seismic data. Unit I, the deepest unit, is interpreted as a lag deposit that infills a topographic low associated with an abrasion platform. Unit I thins seaward by downlap and pinches out landward against the shoreline cutoff. Unit II is a mid-shelf lag deposit formed from shallower eroded material and thins seaward by downlap and landward by onlap. The youngest, Unit III, is interpreted to represent modern sediment deposition. Faults in the study area do not appear to offset the transgressive surface. The Newport Inglewood/Rose Canyon fault system is active in other regions to the south (e.g., La Jolla) where it offsets the transgressive surface and creates seafloor relief. Several shoals observed along the transgressive surface could record minor deformation due to fault activity in the study area. Nevertheless, our preferred interpretation is that the shoals are regions more resistant to erosion during marine transgression. The Cristianitos fault zone also causes a shoaling of the transgressive surface. This may be from resistant antecedent topography due to an early phase of compression on the fault. The Cristianitos fault zone was previously defined as a down-to-the-north normal fault, but the folding and faulting architecture imaged in the CHIRP data are more consistent with a strike-slip fault with a down-to-the-northwest dip-slip component. A third area of shoaling is observed off of San Mateo and San Onofre creeks. This shoaling has a constructional component and could be a relict delta or beach structure.

1. Introduction

Transgressive deposits have been studied along continental margins worldwide and form during a relative sea level rise when rapid increases in accommodation outpace sediment supply (Vail et al., 1977; Van Wagoner et al., 1990; Posamentier and Allen, 1993; Christie-Blick and Driscoll, 1995; Jin and Chough, 1998; Posamentier, 2002; Amorosi et al., 2009; Lantzsch et al., 2009; Nordfjord et al., 2009; Schwab et al., 2014). These deposits are important reservoir rocks for hydrocarbons because they are well sorted and have high permeability (Snedden and Dalrymple, 1999; Posamentier, 2002; Cattaneo and Steel, 2003). Changes in the rate of sea level rise and sediment supply during the transgression imparts both along and across margin variability in the stacking patterns and facies distribution of transgressive deposits (Swift, 1968; Posamentier and Allen, 1993; Cattaneo and Steel, 2003; Catuneanu et al., 2009). Understanding this along and across margin variability of transgressive deposits; however, remains limited because of data quality and density (Nordfjord et al., 2009). A notable exception is the transgressive deposits along the trailing New Jersey/New York margin (e.g., Rampino and Sanders, 1981; Milliman et al., 1990; Greenlee et al., 1992; Miller et al., 1998; Goff et al., 1999, 2004; Nordfjord et al., 2009; Goff and Duncan, 2012; Schwab et al., 2014).

Continental shelves have been exposed to wave-based erosion for the last 2.7 my as sea level has fluctuated up and down ~125 m on a 100–125 ky glacial–interglacial cycle (Petit et al., 1999; Lisiecki and Raymo, 2005). Fluctuations in the rate of eustatic sea level rise since

* Corresponding author.
E-mail address: sklotsko@ucsd.edu (S. Klotsko).

http://dx.doi.org/10.1016/j.margeo.2015.08.003
0025-3227/

the Last Glacial Maximum (LGM; ~21 kya) are well documented (Fairbanks, 1989; Bard et al., 1990; Fairbanks, 1990, 1992; Shackleton, 2000; Peltier and Fairbanks, 2006), with the most rapid rises associated with Melt Water Pulse 1A and Melt Water Pulse 1B (MWP 1A and 1B). During these melt water pulses, rates of eustatic sea level rise topped out at ~40 mm/ky (Hogarth et al., 2012). In between these periods of rapid rise are times of slower sea level rise or even stillstands. These changes in rates of sea level cause different morphologic expressions along and across the margin during the transgression. For example, during slow rises in sea level, there is a greater period of time for wave-base erosion at certain water depths forming abrasion platforms (i.e., terraces). These terraces create localized lows across the shelf that can subsequently be infilled by coarse-grained transgressive lag deposits resulting in thickness and grain size variability (Hart and Plint, 1993; Cattaneo and Steel, 2003). Near sediment dispersal systems, localized prograding packages may develop during these periods of slow sea level rise within the overall backstepping architecture of the transgressive deposit (Posamentier and Allen, 1993; Cattaneo and Steel, 2003). This temporary situation where sediment supply outpaces the relative sea level rise is referred to as a stepped transgressive surface (Swift et al., 1991; Cattaneo and Steel, 2003).

Here we present a high resolution CHIRP survey, together with reprocessed multi-channel seismic data (MCS) from San Onofre, southern California where we define the along and across-margin variability in transgressive deposits in response to changes in the rate of sea level rise and sediment supply. The data also reveal the importance of pre-existing physiography associated with relict tectonic deformation in controlling sediment dispersal and thickness variations of the transgressive deposits (e.g., Posamentier and Allen, 1993; Cattaneo and Steel, 2003). Finally, we present new constraints on local faults (e.g., Newport Inglewood/Rose Canyon and Cristianitos Faults) in high resolution, leading to new conclusions about their deformational style and timing of the most recent earthquake along the faults, which has important implications for geohazard assessment. For example, the deformation and folding style of the Cristianitos Fault, which crosses through the survey area, reveal there is compression across the fault; the fault style and geometry are more consistent with a strike slip fault with a dip-slip component than purely a normal fault as previously proposed (Shlemon, 1992). In summary, high-resolution seismic imaging on continental margins can reveal the across and along margin variability of the transgressive deposit and provide important constraints on the dominant processes through time.

2. Regional setting

2.1. Study area and geologic background

San Onofre is located in seismically active southern California between San Clemente and Oceanside, north of San Diego (Fig. 1A and B). This region offshore is known as the Inner California Continental Borderlands (ICB), a highly deformed portion of the margin (Ehlig, 1977; Crouch, 1979; Legg, 1991; Crouch and Suppe, 1993; Magistrale, 1993; Nicholson et al., 1994; Bohannon and Geist, 1998; Meade and Hagar, 2005; Ryan et al., 2009, 2012). The section of the borderlands that encompasses San Onofre, from Dana Point to Carlsbad Canyon (Fig. 1A), is also characterized by a wider continental shelf than the surrounding area. Onshore, the sea cliffs are composed of four major geologic units at beach level (Fig. 1C). Exposed in the northern part of the region (Fig. 1C) and buried to the south is the San Onofre Breccia, which formed from early to middle Miocene. This is composed of bolder-sized clasts in a finer-grained matrix. Clasts are commonly blue schist, green schist, and quartz schist (Ehlig, 1977). The Monterey Formation (Fm) is exposed in the cliff at beach level south of the Cristianitos Fault (Fig. 1C). This is a deep marine deposit, formed from middle to late Miocene (Ehlig, 1977). The lithology of the formation ranges laterally along the coast from bedded siltstone and clayey siltstone, to interbedded siltstone and biotite-rich sandstone (Ehlig, 1977). The bedded sections of the formation were likely deposited by pelagic sedimentation in an anoxic environment, consistent with the lack of observed bioturbation. At beach level, the cliffs north of the Cristianitos fault zone are composed of the San Mateo Fm, a massive, coarse-grained arkosic sandstone deposited in the late Miocene/early Pliocene (Ehlig, 1977). It is of marine origin and is likely backfill of a channel extending offshore from San Mateo and San Onofre creeks. Toward the southern end of the survey region, the cliffs transition to a coarse-grained arkosic sandstone, which has been previously designated as sandy Monterey Fm (Ehlig, 1977; Kennedy, 2001). Based on grain size evidence and new observations, Sorenson et al. (2009, unpublished UCSD senior thesis) concluded that the grain size distribution is more consistent with the San Mateo Formation. Evidence for a previously undocumented fault with down to the southeast slip would allow for the transition back to San Mateo Formation from Monterey Formation. North of San Mateo and San Onofre creeks, the Capistrano Fm is exposed at beach level in the Capistrano Embayment (Fig. 1C). The Capistrano Fm formed from late Miocene to Early Pliocene and is composed of bedded siltstone, mudstone, and sandstone (Ehlig, 1977), with cemented conglomerate sandstone in marine channels (Kennedy and Tan, 2005). The large clasts are made up of volcanic, metamorphic and sedimentary rocks. Overlying these formations is a reddish-brown Quaternary alluvium deposit. Cut into these deposits is a set of marine terraces. Pebble and cobble gravel lag cover lower terraces, while the upper terraces have more beach sand (Ehlig, 1977). The terraces are thought to have formed during the Pleistocene from eustatic sea level variations and have since been uplifted by tectonic processes (Ehlig, 1977).

2.2. Major faults

The major fault that crosses through the San Onofre region is the Cristianitos (Fig. 1C), a north–northeast trending fault that extends offshore (Ehlig, 1977), coinciding with widest part of the shelf here. The fault is exposed at the coast, where it separates the San Mateo and Monterey formations. There, its strike is 32° northeast and the dip is 58° northwest (Ehlig, 1977). A possible splay of the Cristianitos Fault was identified by Sorenson et al. (2009) ~2.5 km south of where the main fault trace is exposed in the cliff (Fig. 1C). Based on microfossil ages from the Monterey and Capistrano formations, the Cristianitos Fault formed ~10 Ma (Ehlig, 1979). The minimum age of the last rupture has been placed at 125 ka (Marine Isotope Stage 5e; MIS5e) from exposed marine terraces (Shlemon, 1992), but it could be as young as the MIS5a terrace (~80 ka). Paleoseismic trench analysis yields older estimates for the most recent event (MRE) of ~500 ka (McNey, 1979). The Cristianitos Fault has previously been defined as a normal fault (Ehlig, 1977, 1979; Shlemon, 1992), but here, we present evidence suggesting its geometry and deformational style are more consistent with a strike-slip fault with a down-to-the-northwest component.

The major fault along the continental shelf in this region is the Newport Inglewood/Rose Canyon Fault (NI/RC; Fig. 1C), the junction of the Newport Inglewood Fault to the north and the Rose Canyon Fault to the south. It is a right-lateral strike-slip fault that trends northwest–southeast in the survey area along the shelf edge; along some portions of the margin the NI/RC fault delineates the shelf break and in other regions it is within the shelf (Ryan et al., 2009). The Newport Inglewood Fault has been active since at least the Miocene (Freeman et al., 1992). It ruptured multiple times in the 1900s, including a magnitude 6.3 (M_w), highly destructive earthquake in Long Beach. The slip rate for the Newport Inglewood Fault is estimated to be 0.5 mm/yr (Freeman et al., 1992). The Rose Canyon Fault, which formed in the late Pliocene (Ehlig, 1980; Grant et al., 1997), has ruptured at least three times in the past 8.1 ka based on paleoseismic excavations (Lindvall and Rockwell, 1995). The youngest rupture could have occurred as recent as the past few hundred years

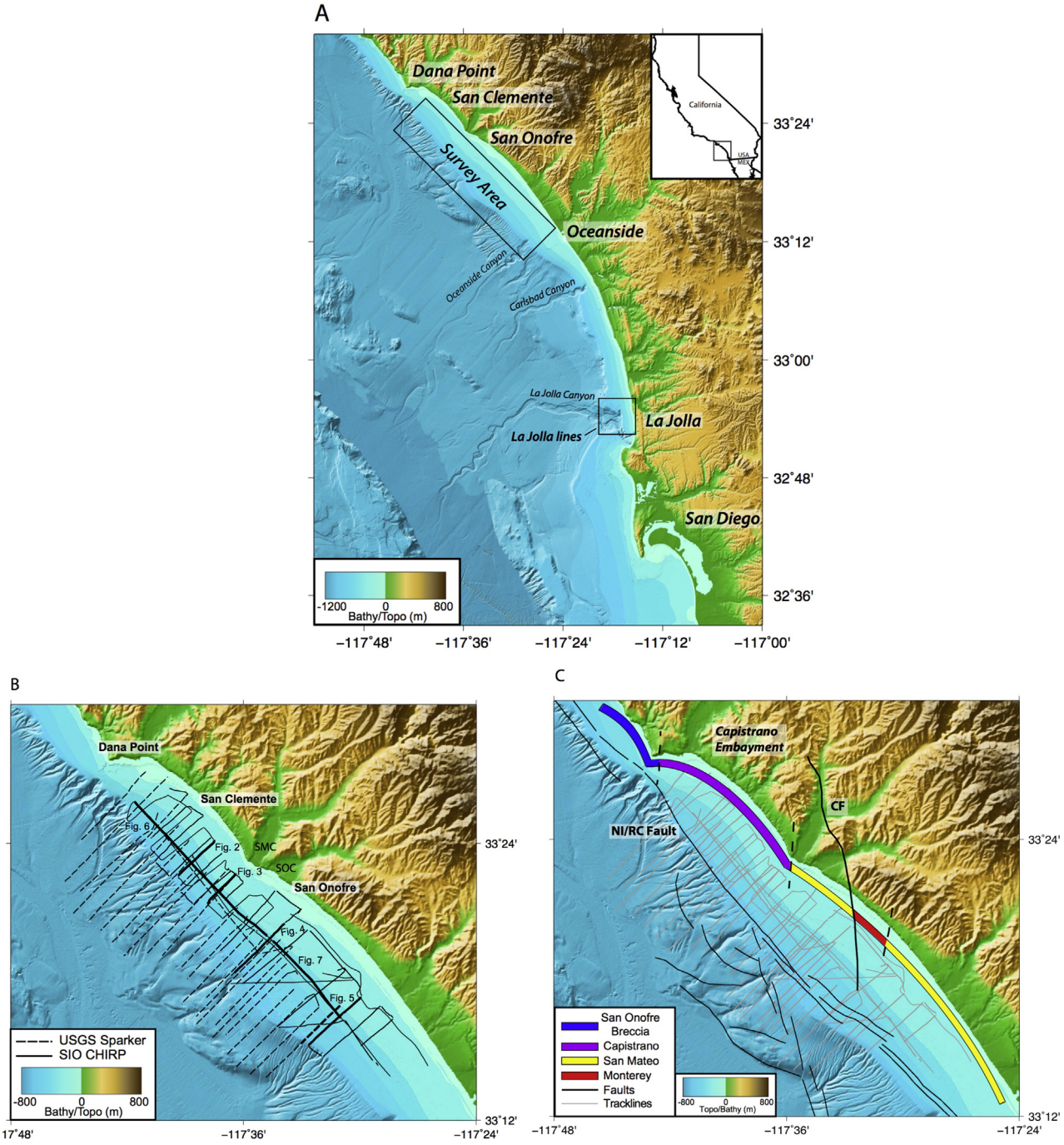

Fig. 1. (A) Regional map of southern California showing the study region from Dana Point to La Jolla Cove. (Inset of California showing map location.) Bathymetry is modified from Dartnell et al. (2015). Large box shows the main study area offshore San Onofre and the small box shows the location of CHIRP lines from La Jolla shown in Fig. 10. (B) Location map for 2008, 2009, and 2013 SIO CHIRP surveys along with USGS mini sparker survey (Sliter et al., 2010). CHIRP tracklines are shown in solid black lines and USGS sparker tracklines are shown in black dashed lines. Seismic lines shown in this paper are bold with labeled figure number. SMC = San Mateo Creek and SOC = San Onofre Creek. (C) Cliff geology and fault map for survey area. Faults are shown in black. Offshore faults are from the USGS fault database and the Cristianitos Fault is based on this study (offshore) and Ehlig (1977; onshore). Geologic formations exposed in the sea cliffs at beach level are shown (Ehlig, 1977; Sorenson et al., 2009; Rentz, 2010). NI/RC = Newport Inglewood/Rose Canyon Fault; CF = Cristianitos Fault.

(Rockwell, 2010). Estimates for the Rose Canyon fault slip rate are between 1 and 2 mm/yr (Lindvall and Rockwell, 1995).

3. Methods

In 2008, 2009, and 2013 CHIRP seismic data were acquired on the continental shelf offshore of San Onofre, CA (Fig. 1) using the Scripps Institution of Oceanography EdgeTech X-Star CHIRP subbottom reflection sonar with sub-meter vertical resolution. The CHIRP system was towed 1–2 m below the surface. Profile spacing ranges from ~0.5 to 2 km. The profiles were acquired using an acoustic source with either a 50 ms, 1–6 kHz or a 30 ms 1–15 kHz swept frequency acoustic source, which allowed for sub-seafloor penetration up to 50 m. All data were recorded in jsf format with real-time GPS navigation recorded with each shot for location accuracy. The data were converted to SEG-Y format and further processed using SIOSEIS (Henkart, 2003) and then imported into IHS Kingdom Suite software package (kingdom.ihs.com) for interpretation. USGS single-channel mini sparker data (Sliter et al., 2010) were reprocessed and imported into Kingdom Suite to increase data density as well as provide deeper seismic imaging. Kingdom Suite was

used to calculate depth to determined surfaces, and layer thicknesses. Generic Mapping Tools (GMT; gmt.soest.hawaii.edu/) were used to apply a continuous curvature surface algorithm and interior tension of 0.35 to convert data points to interpolated grid surfaces. Depth values were calculated using a nominal velocity of 1500 m/s to convert from two way travel time (TWTT); both depth and TWTT are shown on the seismic profiles (Figs. 2–7).

4. Results

4.1. Regional unconformity

A high amplitude subsurface reflector is observed throughout the survey area; it separates truncated horizons and dipping reflectors below from more flat-lying acoustically transparent units above (Fig. 2). This regional unconformity is generally the highest amplitude sub-seafloor reflector; however, it does exhibit lateral amplitude variability. This regional unconformity predominantly shoals from west to east across the study area, ranging from ~75 m to 10 m depth below modern sea level. Abrupt changes in depth and dip along the regional unconformity are observed (Figs. 3 and 4). In particular, there is a marked change in dip at about 53 m below the sea surface from ~0.8° to ~1.77° (Figs. 2 and 3). Furthermore, the regional unconformity exhibits local shoaling across- and along-shelf (e.g., Figs. 5, 6, and 7). Areas of shoaling along the erosion surface in the CHIRP data often appear to correlate spatially with regions of faulting or folding beneath the regional unconformity observed in the mini sparker data (Figs. 5 and 7).

Beneath the regional unconformity the character of the truncated reflectors changes across the shelf and several folds (i.e., antiforms and synforms) are observed. Small fault traces are identified by offsets of the truncated reflectors (Figs. 2 and 3); however, no offsets above the regional unconformity are observed. In addition, below the regional unconformity there are several features that have channel like characteristics (i.e., sediment infill, truncation; Fig. 2). On the southwestern end of most of the dip lines, there is a sequence of subparallel high amplitude reflectors with variable dip in water depths ranging from ~70 m to 115 m that are truncated by the regional unconformity (e.g., Figs. 2 and 3). The gradient of the features appears to steepen toward the west, approaching the shelf edge.

4.2. Acoustic units

There are three well-defined sedimentary units above the regional angular unconformity (Figs. 2 and 3). The basal unit, Unit I, lies directly above the regional unconformity. It infills a structural low seaward of a change in the slope of the regional unconformity at ~53 m below current sea level (Figs. 2 and 3). This unit predominantly occurs in water depths ranging from ~40 to 75 m and onlaps landward and downlaps seaward. In the region of onlap, the reflector amplitude is high and systematically diminishes offshore, where it becomes acoustically blotchy and discontinuous (Fig. 3). The isopach map for Unit I (Fig. 8A) shows the thickness depocenter is offshore San Mateo and San Onofre creeks (~12 m thick) in water depths >40 m. Throughout the rest of the survey area, the thickness of Unit I is less than ~5 m. A marked increase in thickness occurs along the mid-shelf (~40–60 m present water depth) where the slope of the regional unconformity increases (Fig. 3).

In addition to onlapping the regional unconformity across the margin (Fig. 2), Unit I exhibits lateral onlap onto a shoal in the regional unconformity (Fig. 6). A different acoustic character in Unit I is observed on either side of the local shoal. A mounded structure is observed above the regional unconformity in this region, which has a high acoustic reflectivity and relief (purple package in Fig. 6). Despite the fact that Unit I characteristically infills structural lows and diminishes relief, this mounded structure is included in the isopach map for Unit I (Fig. 8A) because it appears to be a laterally time-equivalent facies and it is overlain by Unit II (Fig. 6). South of the mound structure (Fig. 7), Unit I exhibits lateral onlap onto another local shoal on the regional unconformity (Fig. 7). In contrast to the northern shoal (Fig. 6), the reflectors beneath the regional unconformity in this region are folded and faulted (Fig. 7).

Unit II overlies Unit I, or the regional unconformity where Unit I is absent (Figs. 2–5). In the seismic data, it has a lenticular shape and is observed in water depths ranging between ~20 and 70 m, pinching out by either onlap landward or downlap seaward. The top of the unit

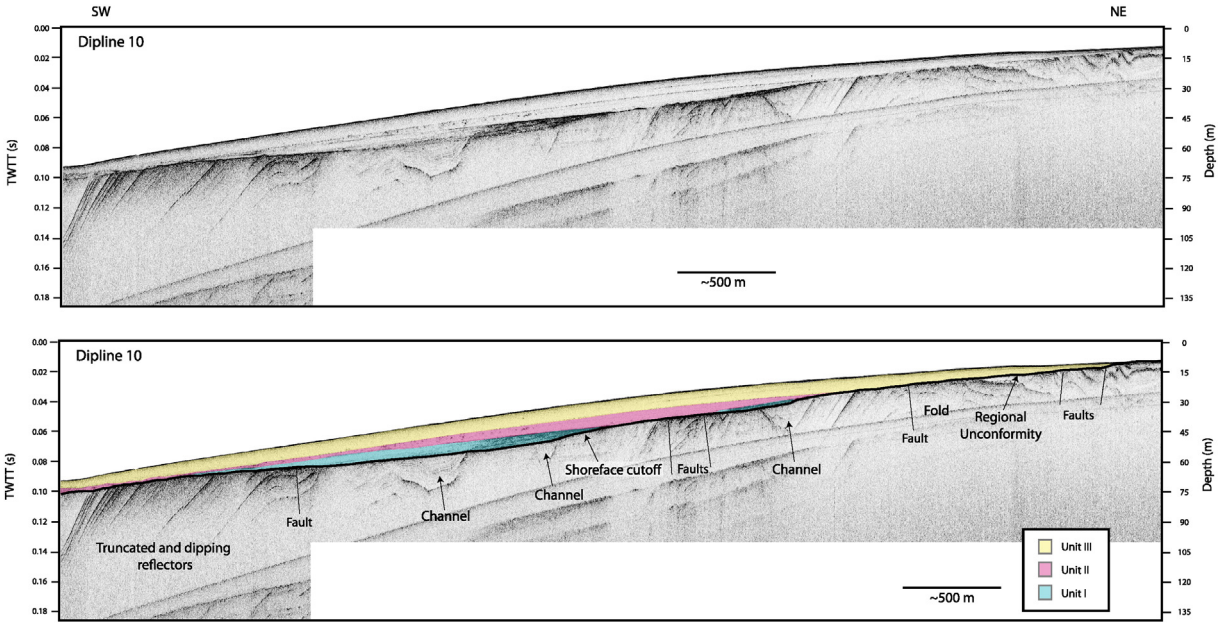

Fig. 2. CHIRP dipline 10 with uninterpreted (Top) and interpreted (Bottom) versions. Unit I is shown in cyan, Unit II is shown in pink, and Unit III is shown in yellow. Several folds and faults are observed beneath the transgressive surface, but do not appear to offset it. Unit I is observed at midshelf depths and thins by onlap landward and downlap seaward. Unit II is shifted landward with respect to Unit I. Both Units I and II are overlain by Unit III. (For interpretation of the references to color in this figure legend, the reader is referred to the web version of this article.)

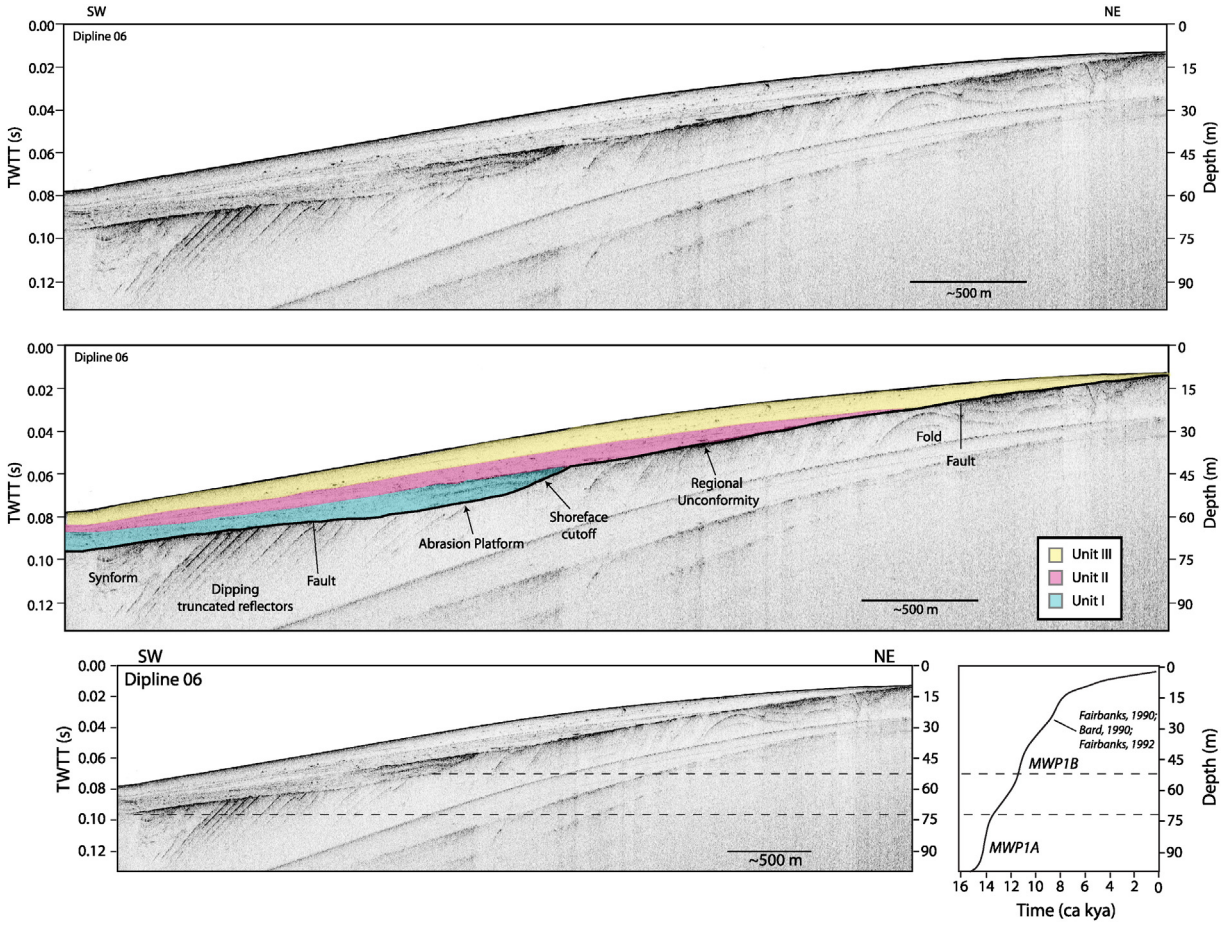

Fig. 3. CHIRP dipline 06 with uninterpreted (top) and interpreted (middle) versions. Along the southwestern portion of the profile, there is pronounced truncation beneath the transgressive surface. Moving toward the northeast along the abrasion platform is a marked change in relief, which is interpreted as a shoreface cutoff. The stacking patterns of Units I, II, and III exhibit a similar pattern as observed in CHIRP dipline 10. The bottom CHIRP profile is shown with the LGM sea level curve based on Fairbanks (1990), Bard et al. (1990), and Fairbanks (1992). The decrease in the rate of sea-level rise following MWP 1A correlates with the deeper portion of the abrasion platform; the upper depth limit correlates to the increase in sea-level rise associated with MWP 1B. The more rapid rise at MWP 1B also allows the shoreline cutoff to be preserved as wave-base erosion moved landward. Dashed lines show the decreased rate of sea level rise between MWP 1A and MWP 1B and associated depth corridor on the shelf.

is delineated by a faint acoustic reflector, which can be traced throughout most of the study region (Figs. 3, 4, and 7). This unit contains some internal reflectors, which are discontinuous and variable in amplitude (Figs. 2 and 3). An isopach map of Unit II (Fig. 8B) shows that the thickest deposits (~12 m thick) are along the center of the survey offshore the San Mateo and San Onofre creeks similar to the depocenter for Unit I. Nevertheless, the depocenter for Unit II is located eastward (~15–45 m water depth) with respect to the depocenter for Unit I (Fig. 8A and B).

Unit III is the uppermost unit and blankets most of the study area. It is mostly acoustically transparent, but includes some discontinuous, low amplitude, reflectors. Unit III thins landward and is absent toward the east where the regional unconformity is exposed at the seabed (e.g., Figs. 2 and 4). The isopach map for Unit III (Fig. 8C) shows its broad regional extent, which systematically thickens offshore reaching a maximum thickness of ~10 m near the mid-shelf (~30–40 m water depth), where it then thins seaward (Fig. 8C).

5. Discussion

5.1. Transgressive surface

The regional unconformity observed throughout the data is interpreted to be the transgressive surface formed by wave-base erosion as sea level rose following the LGM (Posamentier and Allen, 1993; Le Dantec et al., 2010; Hogarth et al., 2012). This boundary is defined by truncation and onlap; by inference it separates deposits exposed subaerially during the LGM below from marine deposits above. Channels are observed beneath the transgressive surface, and are interpreted to have formed during the last glacial maximum by fluvial incision and downcutting. As previously mentioned, the transgressive surface shows a change in dip at ~53 m below sea level from ~0.8° to ~1.77°. This change in dip is interpreted to be the boundary between the wave-cut abrasion platform and the shoreline cutoff (Figs. 3 and 9; e.g., Posamentier and Allen, 1993; Muhs et al., 1994). The deepest abrasion platform is observed at water depths of 72–53 m (Figs. 2 and 3). Based on water depth and no tectonic uplift, this abrasion platform appears to be cut during the slowdown in sea level rise between MWP 1A and MWP 1B (Fig. 3; Bard et al., 1990, 1996; Fairbanks, 1990, 1992). The rate of sea level rise is up to ~40 mm/yr for MWP 1A and MWP 1B and diminishes to ~8 mm/yr during the intervening decrease in sea level rise (Hogarth et al., 2012). This slow down allowed for a longer period of wave-base erosion creating a pronounced shoreline cutoff observed along the shelf in our study area (Fig. 3). In our conceptual model, Unit I was deposited after MWP 1B as the abrasion platform moved landward (Fig. 9B). The eroded sediment is then advected landward and seaward, with the coarse transgressive lag infilling the relief on the transgressive surface (Unit I; e.g., Hogarth et al., 2012). Such an interpretation is consistent with the high amplitude reflectors that onlap the shoreline cutoff (Figs. 2 and 3). The top

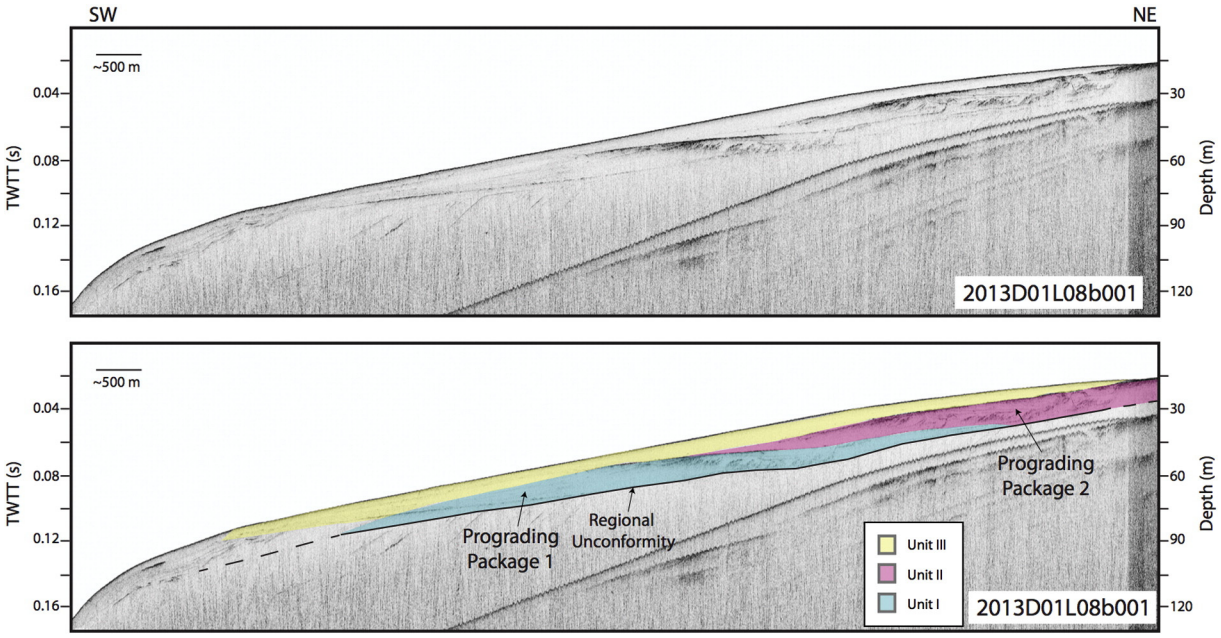

Fig. 4. 2013 dipline D01L08b001 with uninterpreted (top) and interpreted (bottom) versions. The transgressive surface is shown in black, and is dashed where uncertain. Prograding package 1 is shown in cyan and is associated with Unit I. Prograding package 2 is shown in pink and is associated with Unit II. Near San Mateo and San Onofre creeks the sediment supply after MWP 1B outpaces the eustatic rise and the unit progrades. Likewise package 2 progrades after ~8 ka, when sediment supply outpaces new accommodation. (For interpretation of the references to color in this figure legend, the reader is referred to the web version of this article.)

of the infilling lag deposit (Unit I) has a similar dip to the shallower abrasion platform (Figs. 3 and 9B), with deposition occurring below wave base. The isopach maps show the important control on shelf sediment thickness by the shoreline cutoff (Fig. 8). The depocenter for Unit I occurs just to the west of the shoreline cutoff (Fig. 8A), with the depocenter for Unit II occurring just east of this (Fig. 8B). These

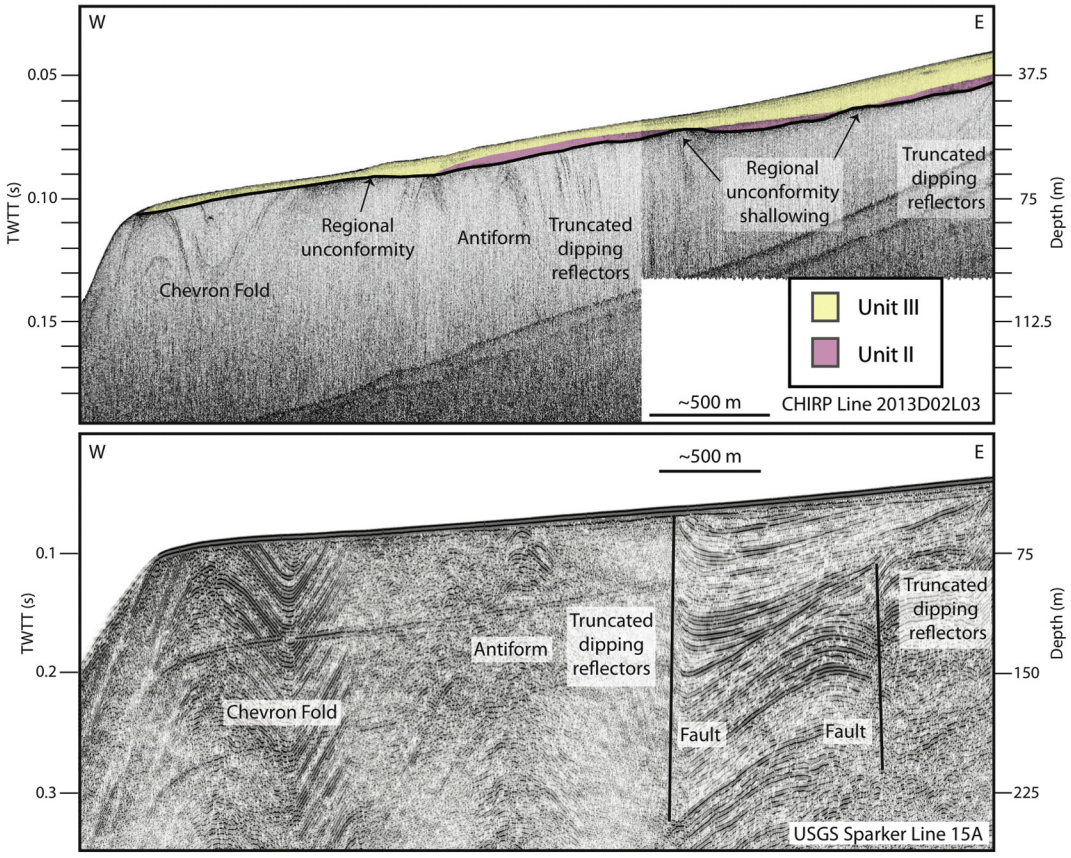

Fig. 5. Comparison of 2013 SIO CHIRP line D02L03 (top) and USGS mini sparker line 15A (bottom). On the CHIRP profile, Unit II is shown in pink, and Unit III is shown in yellow. Faults observed in the sparker data correspond with regions of shoaling along the transgressive surface imaged in the CHIRP data. (For interpretation of the references to color in this figure legend, the reader is referred to the web version of this article.)

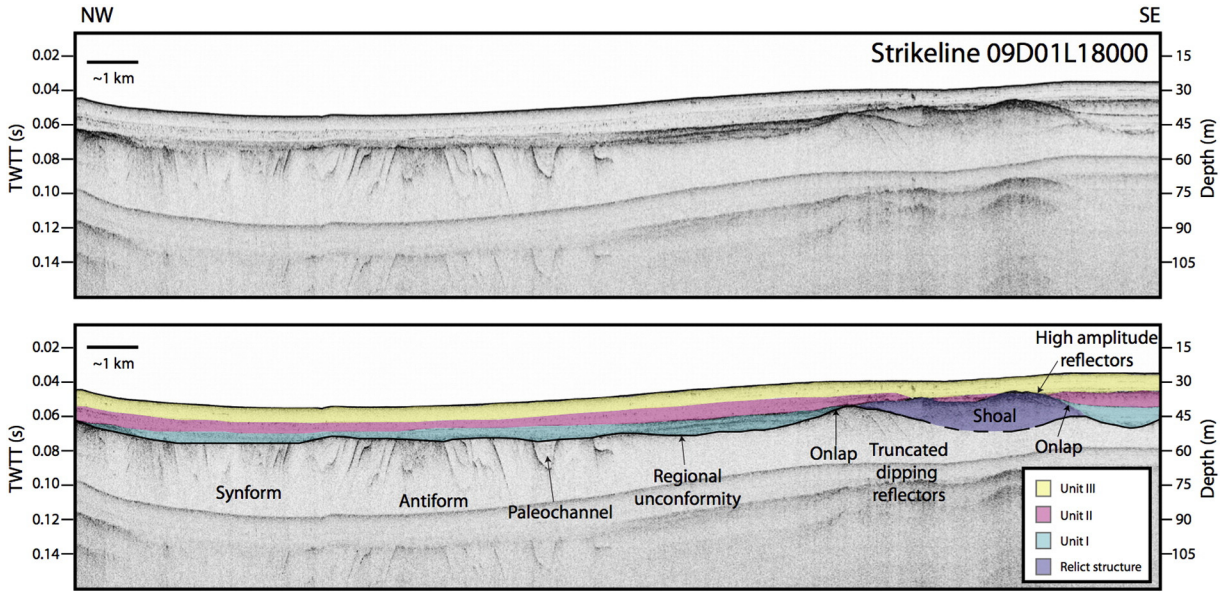

Fig. 6. CHIRP strikeline 18 with uninterpreted (top) and interpreted (bottom) versions. Shown in purple is an interpreted relict beach or delta structure, sediment was likely sourced from the San Mateo and San Onofre creeks. (For interpretation of the references to color in this figure legend, the reader is referred to the web version of this article.)

depocenters occur off of San Mateo and San Onofre Creeks where the sediments were actually able to outpace the transgression and prograded out (Fig. 4).

In addition to the relief and control of across shelf sediment thickness by the submerged relict shoreline cutoff (Kern and Rockwell, 1992), there are along-strike shoals that also control shelf sediment dispersal and thickness (Figs. 6 and 7). The northern shoaling region occurs offshore San Mateo and San Onofre creeks. This shallowing region is composed of two close shoals in the transgressive surface with truncated dipping reflectors below (Fig. 6). In this region, it is unclear why there is differential relief along the transgressive surface, but topography resistant to erosion could be a potential cause. Above these shoals in the transgressive surface is a high amplitude constructional sediment unit that post-dates the formation of the transgressive surface as evidenced by the observed truncation of reflectors at the transgressive surface (purple package in Fig. 6). This sedimentary package creates relief and is interpreted as a relict beach or delta deposit formed from sediment supply from the San Onofre and San Mateo Creeks. Unit I is younger than this constructional sediment package based on the observed onlap of Unit I onto this feature (Fig. 6). A few kilometers northwest of the shoal, a tight zone of folding and deformation is observed beneath the transgressive surface (Fig. 6) and correlates with a facies change observed in the sea cliffs at beach level from San Mateo Formation (Fm) to the south and Capistrano Fm toward the north (Fig. 1C; Rentz, 2010). This zone of deformation projects onshore to the southern end of the Capistrano Embayment (Ehlig, 1979) and potentially correlates with a down-to-the-northwest strike-slip fault (Rentz, 2010). We interpret this deformation zone to be a northern splay of the Cristianitos Fault. The down-to-the-northwest Cristianitos Fault and the down-to-the-northwest splay explain the formations exposed in the sea cliffs being younger to the north. At Dana Point, the strike slip fault system reverses and is down-to-the-northeast, which

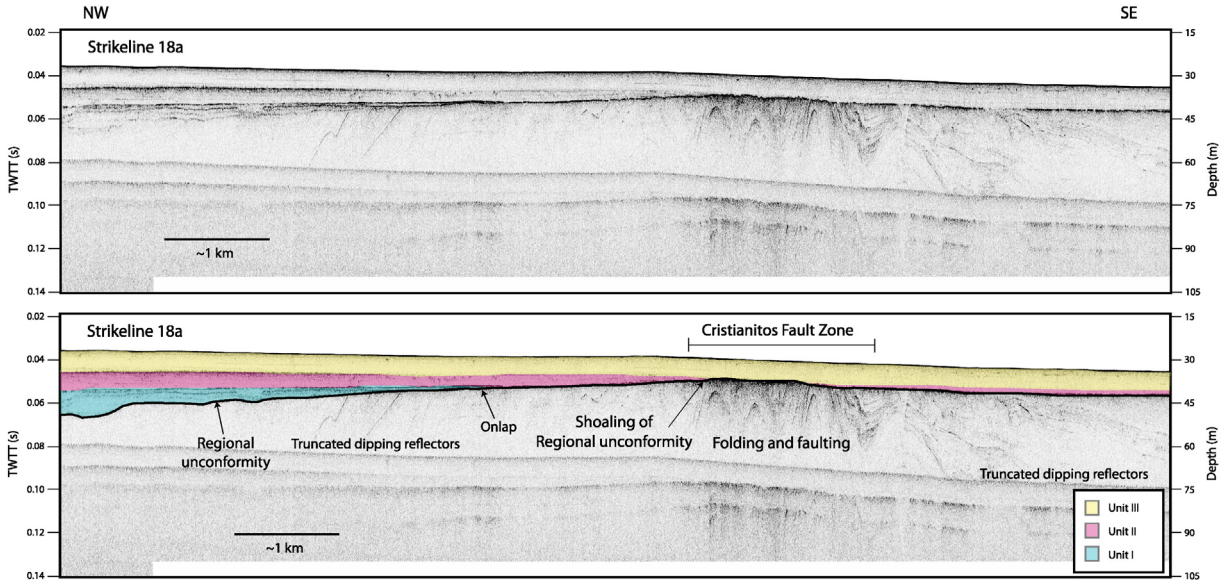

Fig. 7. CHIRP strikeline 18a with uninterpreted (top) and interpreted (bottom) versions. The Cristianitos fault zone corresponds to the region of folding and faulting observed beneath the transgressive surface.

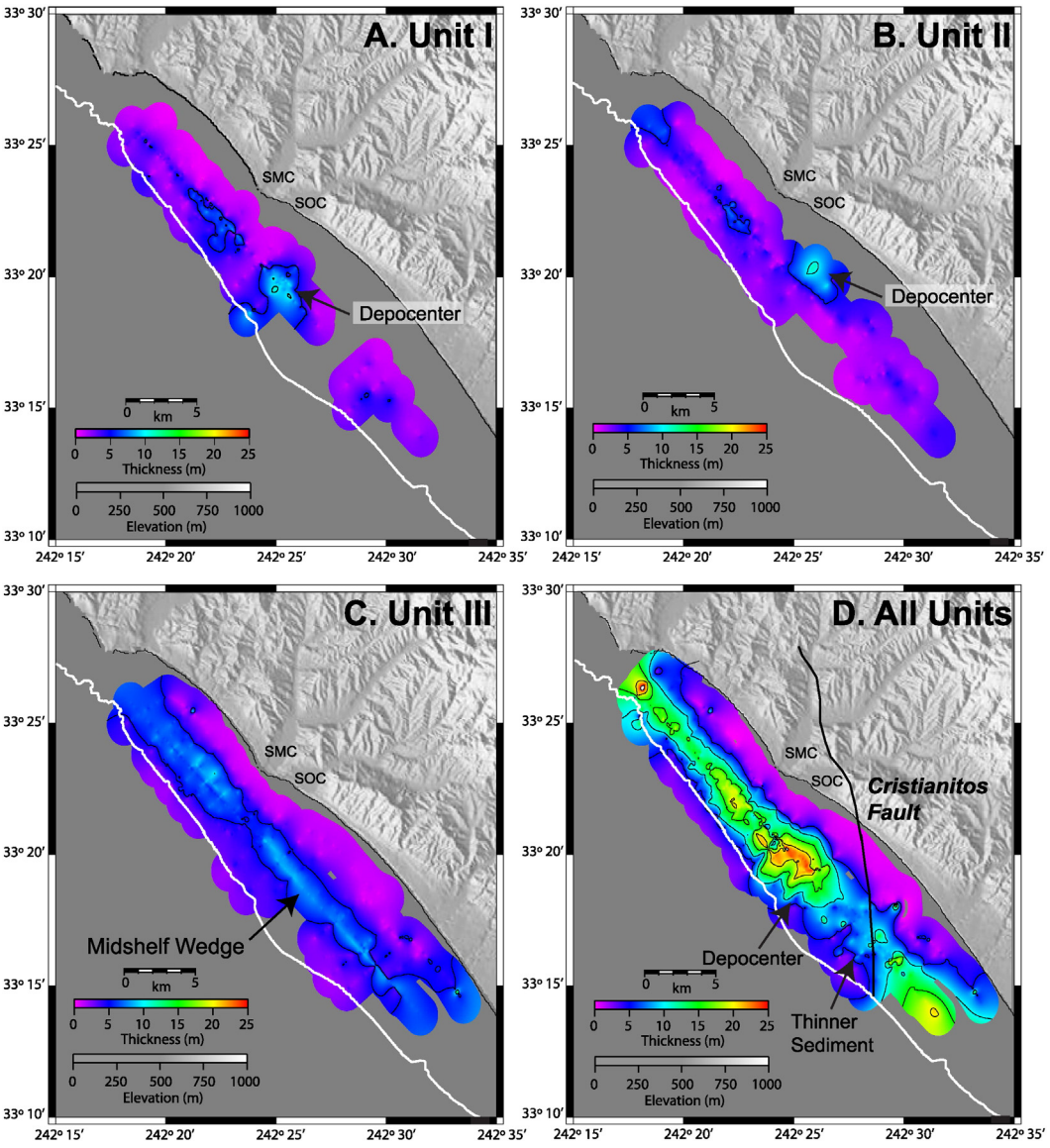

Fig. 8. Sediment thickness maps. (A) Unit I, (B) Unit II, (C) Unit III, (D) total sediment thickness from transgressive surface to seafloor. Maps show the 100 meter bathymetric contour in white. 5 meter contours of layer thickness are shown by thin black lines. SMC = San Mateo Creek and SOC = San Onofre Creek. Notable features are labeled.

juxtaposes the older San Onofre Breccia to the north against the younger Capistrano Fm (Fig. 1C).

Farther south, another region of folding and deformation is observed beneath the transgressive surface (Fig. 7), which correlates with a structural high on the transgressive surface. The trace of this deformation projects landward to the Cristianitos Fault, which is interpreted onshore to be a down-to-the-northwest normal fault as it separates older Monterey Fm to the south from younger San Mateo Fm (Fig. 1C; Ehlig, 1977, 1979; Shlemon, 1992). The identification of the Cristianitos Fault is also supported by the difference in seismic character on either side of the fault zone, which is analogous to the onshore deposits (Figs. 1C and 7). The San Mateo Fm is a blocky, homogenous sandstone, which may explain the lack of reflectors observed in the CHIRP profiles. South of the fault, the dipping reflectors appear to be caused by impedance contrasts in the Monterey Fm, a claystone with layers of indurated porcelanite. The folding and faulting observed beneath the transgressive surface, associated with the Cristianitos fault zone, is more consistent with a strike-slip fault with a down-to-the-northwest dip-slip component. Despite the observed deformation, there is no clear offset of the transgressive surface (Fig. 7). This shoal either records deformation (uplift) since the erosion of the transgressive surface or antecedent topography that was more resistant to wave-base erosion. Onshore a transgressive lag/abrasion platform, interpreted to be formed during either Marine Isotopic Stage (MIS) 5A (80 ka) or (MIS) 5E (125 ka), is not offset across the Cristianitos Fault (Shlemon, 1992). Therefore, our preferred hypothesis is that the shoal on the transgressive surface is resistant antecedent topography.

Other shoals along the transgressive surface correlate with the Newport Inglewood/Rose Canyon (NI/RC) fault (Figs. 1C and 5). Nested geophysical sparker and CHIRP profiles allow us to examine the deformation and stratigraphy across a variety of spatial and temporal scales. The two faults identified in the sparker data correlate with shoals observed in the CHIRP data. Moreover, there is no observed offset of the transgressive surface across the shoal. Note that the folds observed in the sparker data can be observed beneath the transgressive surface in the CHIRP data (Fig. 5). In this region, it is possible that recent NI/RC fault deformation has little to no vertical component of slip and thus would be difficult to image in the CHIRP data; however, at depth beneath the transgressive surface in the sparker data, a vertical component of slip with folding is observed across the NI/RC fault zone (Fig. 5).

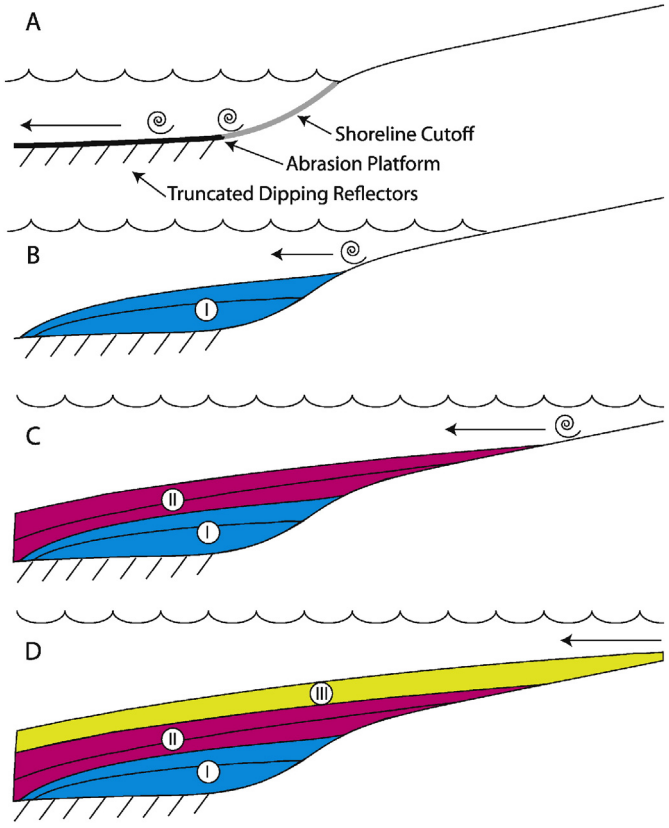

Fig. 9. Formation of a marine terrace. Swirls represent location of erosion of seafloor. (A) When the rate of sea-level rise diminishes, the corresponding depth corridor is exposed to a longer period of wave-base erosion and formation of the abrasion platform. The eroded sediment is transported both onshore and offshore. (B) As the rate of sea level rise increases, the depth corridor exposed to wave-base erosion migrates landward and the eroded material is transported landward and seaward. Coarse-grained sediment infills the relief associated with the previous abrasion platform and shoreline cutoff. This infilling lag deposit (Unit I) is shown in cyan. (C) With continued sea-level rise, the wave-base erosion continues to move landward with eroded material being transported landward and seaward. This midshelf lag deposit (Unit II) is shown in pink. (D) Sea level rises higher and the zone of erosion moves shoreward, with this material transported onshore and offshore. This modern sediment deposit (Unit III) is shown in yellow. (For interpretation of the references to color in this figure legend, the reader is referred to the web version of this article.)

Given the lack of deformation in the high-resolution CHIRP data above the transgressive surface, our preferred interpretation is that the most recent event pre-dates the formation of this surface.

Some deformation and uplift associated with the NI/RC fault (Fig. 5) could post-date the formation of the transgressive surface and be recorded by the onlap of Unit II. Nevertheless, this is not our preferred interpretation based on the following observations. First, the Cristianitos Fault exhibits very similar deformational pattern, creating a shoal on the transgressive surface, but onshore evidence suggests that there has been no slip younger than 125 ky (Shlemon, 1992), implying the fault is inactive. In addition to the south (Fig. 1A), where the Rose Canyon Fault appears active with measured Holocene slip in onshore trench data (Lindvall and Rockwell, 1995), the offshore CHIRP data north of the Rose canyon images deformation of the transgressive surface and seafloor (Fig. 10). Onshore paleoseismic data in La Jolla yield slip rates of 1–2 mm/yr (Lindvall and Rockwell, 1995), with the Most Recent Event (MRE) occurring in 1650 AD. The previous 5 events appear clustered and occurred between 9.3 and 5 ka (Lindvall and Rockwell, 1995). Farther north along the NI/RC fault, long-term slip rates are estimated at 0.5 mm/yr based on well data from Long Beach and Seal Beach oil fields (Freeman et al., 1992) and 0.34–0.55 mm/yr based on cone penetrometer testing (Grant et al., 1997). These slip rates are less than what has been determined from La Jolla trench sites (1–2 mm/yr; Lindvall and Rockwell, 1995). Unlike the shoaling of the transgressive surface across the Cristianitos Fault, there is no independent age information to determine between the two scenarios mentioned above (transgressive shoal records recent deformation versus antecedent resistant topography). Even though our preferred hypothesis is the shoaling of the transgressive surface in our study area is antecedent topography, we cannot rule out that the shoaling is due to more recent deformation on the NI/RC fault.

5.2. Sediment units

All unit interpretations were based on acoustic character and stratal geometry. Units I, II, and III are interpreted to be an infilling lag deposit, a midshelf lag deposit, and modern sediment, respectively. Unit I is bounded by the transgressive surface below and above by Unit II, where present, or Unit III (Figs. 2 and 3). The backstepping sequence of Units I and II is consistent with the landward migration of sediments associated with sea level rise. Similar uplifted wave-cut terraces are observed onshore in the region with mainly beach gravels, pebbles, and sand deposits (Ehlig, 1977; McNey, 1979; Shlemon, 1992), which record past relative sea level cycles. Likewise, dipping and truncated reflectors observed in the western part of the shelf are interpreted to be prograding units formed during older Pleistocene relative sea-level falls.

Unit II lies primarily between the infilling lag deposit (Unit I) and the modern sediment, but overlies the transgressive surface where Unit I is absent (Fig. 7). The depocenter for Unit II is located landward (shallower) than Unit I (Fig. 8). Even though Unit II is characterized by only a minor increase in acoustic reflectivity and more-gentle onlap, the material was likely sourced and transported seaward to its current location from a shallower abrasion surface (e.g., Figs. 3 and 9). No shoreline cutoff is observed along the landward edge of the abrasion platform. The lack of a shoreline cutoff suggests that the rate of sea-level rise post MWP 1B was more uniform with less abrupt changes in rate (i.e., no evidence for large changes in the rate of sea level rise following MWP 1B; Fairbanks, 1989, 1990; Bard et al., 1990; Fairbanks, 1992; Shackleton, 2000; Peltier and Fairbanks, 2006). Unit III is the result of modern sedimentation that overlies the other units. The unit is acoustically transparent suggesting it is well sorted and homogenous, typical of modern marine deposition on inner-California shelves (Le Dantec et al., 2010; Hogarth et al., 2012).

5.3. Controls on sediment thickness

In regions away from the San Mateo and San Onofre creeks, sediment dispersal is controlled predominantly by variations in the rate of sea level rise. Specific depth corridors along the shelf either experience more or less erosion and reworking if they correlate with slow rates of sea level rise or periods of rapid sea level rise, respectively. For example, the 53–72 m depth corridor corresponds to a diminished rate of sea level rise between MWP 1A and MWP 1B and experienced prolonged wave-base erosion with the formation of a shoreline cutoff (Fig. 3). Other shoals and changes in relief along the transgressive surface (e.g., Cristianitos Fault and NI/RC fault; Figs. 5 and 7) play an important role in controlling the distribution of Unit I and to a lesser extent Unit II (Figs. 5 and 7), which is captured in the isopach maps for these units (Fig. 8A and B). Sediment input from the San Mateo and San Onofre creeks also plays a role in sediment stacking patterns observed in Units I and II (Figs. 4, 6, and 8B). This local source of riverine sediment creates an area of increased supply and enhanced sediment thickness for Units I and II (Fig. 8A, B, and D). In this region, we also observe prograding packages along the margin following MWP 1B and the slowdown in sea level rise after ~8 kya (Fig. 4). Based on the observed stratal geometry and prograding packages, an increase in sediment supply occurs near the San Mateo and San Onofre creeks (Fig. 4). In summary, tectonic deformation along this portion of the southern California

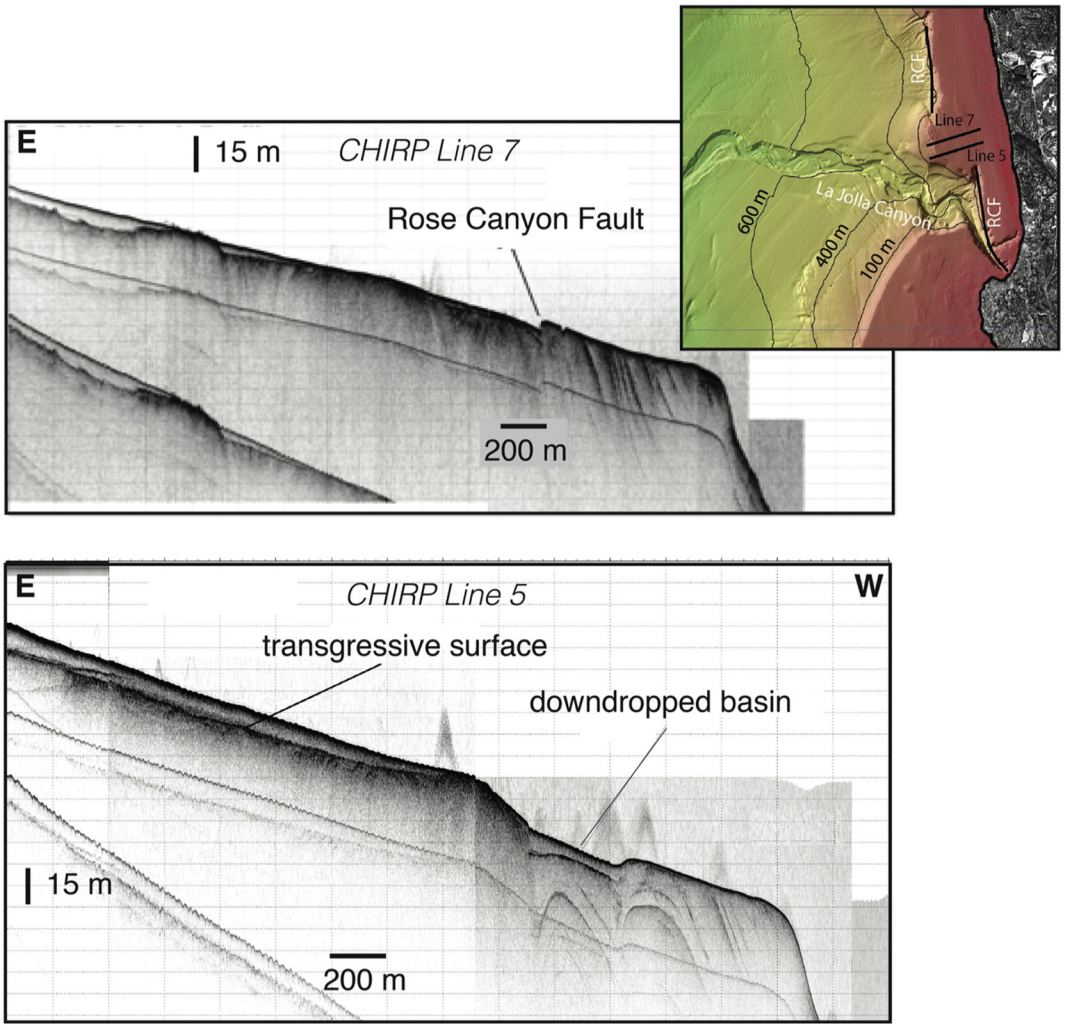

Fig. 10. CHIRP seismic profiles across the Torrey Pine pop-up structure (Hogarth et al., 2007). (Top) Line 7 crosses the Rose Canyon Fault and images a seafloor scarp with ~5 m of relief. (Bottom) Line 5 crosses the Rose Canyon Fault where it is expressed by two strands and creates a down-dropped block between the bounding fault stands. Note the offset of the transgressive surface and the increased sediment thickness across the down-dropped block. Inset shows location of the CHIRP data. RCF = Rose Canyon Fault. Site is also shown in Fig. 1A.

continental shelf plays a subordinate role to rates of eustastic change and sediment supply.

6. Conclusions

Analysis of new high-resolution CHIRP data and USGS mini sparker data has provided information about the factors controlling sediment distribution and facies variations within the transgressive sequence on the continental shelf offshore of San Onofre, CA. The shelf exhibits three depositional units that record the interplay between the rate of eustatic sea level rise and sediment supply. Unit I and Unit II are interpreted as lag deposits, coarser material that was eroded from an abrasion platform. Unit I fills in lows in the transgressive surface and younger Unit II transverses the midshelf. Unit III is acoustically transparent modern marine sedimentation. An observed change in dip of the transgressive surface at ~53 m (moving upslope) was carved by the slowdown in eustatic sea level rise between MWP 1A and MWP 1B. Unit I infills this along-shelf low, with its thickest deposits to the west. A shoaling of the transgressive surface is observed offshore of San Mateo and San Onofre creeks. Enhanced sediment supply from the San Mateo and San Onofre creeks created an extended beach or delta structure in this region (Fig. 6). Other areas of shoaling of the transgressive surface are associated with folding and faulting (Figs. 5 & 7). In regions where folding and faulting beneath the transgressive surface are observed, it is possible that the shoaling occurred after the formation of the transgressive surface, but more likely the shoals are erosion-resistant antecedent topography. The Cristianitos fault zone, where extensive compressional folding is observed, causes one of these shoals (Fig. 7). This leads to the conclusion that the Cristianitos Fault is not a simple normal fault, but is in fact, a strike-slip fault with a down-to-the-northwest component. In this region, local tectonics do not play a major role in sediment distribution, rather rates of eustatic sea level change and local sediment supply appear to be the governing factors. The abrasion platform formed during the still stand between MWP 1A and MWP 1B (Younger Dryas) places important age constraints on the activity for this segment of the NI/RC fault.

Acknowledgments

Support for SK was provided by the National Science Foundation's Graduate Research Fellowship (DGE-1144086). Support for data acquisition and processing was provided by Southern California Edison. Comments from two anonymous reviewers and J.E. Conrad greatly improved the manuscript.

References

Amorosi, A., Lucchi, M.R., Rossi, V., Sarti, G., 2009. Climate change signature of small-scale parasequences from Lateglacial–Holocene transgressive deposits of the Arno valley fill. Palaeogeogr. Palaeoclimatol. Palaeoecol. 273, 142–152.

Bard, E., Hamelin, B., Fairbanks, R.G., Zindler, A., 1990. Calibration of the ^{14}C timescale over the past 30,000 years using mass spectrometric U–Th ages from Barbados corals. Nature 345, 405–409.

Bard, E., Hamelin, B., Arnold, M., Montaggioni, L., Cabioch, G., Faure, G., Rougerie, F., 1996. Deglacial sea-level record from Tahiti corals and the timing of global meltwater discharge. Nature 382 (6588), 241–244.

Bohannon, R.G., Geist, E., 1998. Upper crustal structure and Neogene tectonic development of the California continental borderland. Geol. Soc. Am. Bull. 110 (6), 779–800.

Cattaneo, A., Steel, R.J., 2003. Transgressive deposits: a review of their variability. Earth-Sci. Rev. 62, 187–228.

Catuneanu, O., Abreu, V., Bhattacharya, J.P., Blum, M.D., Dalrymple, R.W., Eriksson, P.G., Winker, C., 2009. Towards the standardization of sequence stratigraphy. Earth Sci. Rev. 92, 1–33.

Christie-Blick, N., Driscoll, N.W., 1995. Sequence stratigraphy. Annu. Rev. Earth Planet. Sci. 23, 451–478.

Crouch, J.K., 1979. Neogene tectonic evolution of the western Transverse Ranges and the California Continental Borderland. Geol. Soc. Am. Bull. 90, 338–345.

Crouch, J.K., Suppe, J., 1993. Late Cenozoic tectonic evolution of the Los Angeles Basin and inner California borderland; a model for core complex-like crustal extension. Geol. Soc. Am. Bull. 105 (11), 1415–1434.

Dartnell, P., Driscoll, N.W., Brothers, D., Conrad, J.E., Kluesner, J., Kent, G., Andrews, B., 2015. Colored shaded-relief bathymetry, acoustic backscatter, and selected perspective views of the inner continental borderland. Geological Survey Scientific Investigations Map 3324, 3 sheets, Southern California, U.S. http://dx.doi.org/10.3133/sim3324.

Ehlig, P.L., 1977. Geologic report on the area adjacent to the San Onofre Nuclear Generating Station, Northwestern San Diego County, California. Neotectonics and Coastal Instability: Orange and Northern San Diego Counties, Californiapp. 113–132.

Ehlig, P.L., 1979. The Late Cenozoic evolution of the Capistrano embayment. In: Fife, D.L. (Ed.), Geologic Guide of San Onofre Nuclear Generating Station and Adjacent Regions of Southern California.

Ehlig, P., 1980. Rose Canyon Fault. Unpublished Report for Southern California Edison, January, 32 pp.

Fairbanks, R.G., 1989. A 17,000 year glacio-eustatic sea level record: Influence of glacial melting rates on the Younger Dryas event and deep-ocean circulation. Paleoceanography 342, 637–642.

Fairbanks, R.G., 1990. The age and origin of the "Younger Dryas climate event" in Greenland ice cores. Paleoceanography 5 (6), 937–948.

Fairbanks, R., 1992. Barbados sea level and Th/U ^{14}C calibration. IGBP PAGES/World Data Center for Paleoclimatology Data Contribution Series # 92-020. NOAA/NGDC Paleoclimatology Program, Boulder CO, USA.

Freeman, S. Thomas, Heath, Edward G., Guptill, Paul D., Waggoner, John T., 1992. Seismic hazard assessment, Newport–Inglewood fault zone. Association of Engineering Geologists, Southern California Section, Special Publication No. 4.

Goff, J.A., Duncan, C.S., 2012. Re-examination of sand ridges on the middle and outer New Jersey shelf based on combined analysis of multibeam bathymetry and backscatter, seafloor grab samples and chirp seismic data. In: Li, M.Z., Sherwood, C.R., Hill, P.R. (Eds.), Sediments, Morphology and Sedimentary Processes on Continental Shelves: Advances in Technologies, Research, and Applications. John Wiley and Sons, Ltd., Chichester, West Sussex, pp. 121–142.

Goff, J.A., Swift, D.J.P., Duncan, C.S., Mayer, L.A., Hughes-Clarke, J., 1999. High resolution swath sonar investigation of sand ridge, dune and ribbon morphology in the offshore environment of the New Jersey margin. Mar. Geol. 161, 309–339.

Goff, J.A., Kraft, B.J., Mayer, L.A., Schock, S.G., Sommerfield, C.K., Olson, H.C., Nordfjord, S., 2004. Seabed characterization on the New Jersey middle and outer shelf: correlatability and spatial variability of seafloor sediment properties. Mar. Geol. 209 (1), 147–172.

Grant, L.B., Waggoner, J.T., Rockwell, T.K., von Stein, C., 1997. Paleoseismicity of the north branch of the Newport–Inglewood fault zone in Huntington Beach, California, from cone penetrometer test data. Bull. Seismol. Soc. Am. 87 (2), 277–293.

Greenlee, S.M., Devlin, W.J., Miller, K.G., Mountain, G.S., Flemings, P.B., 1992. Integrated sequence stratigraphy of Neogene deposits, New Jersey continental shelf and slope: comparison with the Exxon model. Geol. Soc. Am. Bull. 104 (11), 1403–1411.

Hart, B.S., Plint, A.G., 1993. Tectonic influence on deposition and erosion in a ramp setting: upper cretaceous cardium formation, Alberta foreland basin. Am. Assoc. Pet. Geol. Bull. 77, 2092–2107.

Henkart, P., 2003. SIOSEIS, Software. Scripps Institution of Oceanography, La Jolla, CA (available at http://sioseis.ucsd.edu).

Hogarth, L.J., Babcock, J., Driscoll, N.W., Le Dantec, N., Haas, J.K., Inman, D.L., Masters, P.M., 2007. Long-term tectonic control on Holocene shelf sedimentation offshore La Jolla, California. Geology 35 (3), 275–278. http://dx.doi.org/10.1130/G23234A.1.

Hogarth, L.J., Driscoll, N.W., Babcock, J.M., Orange, D.L., 2012. Transgressive deposits along the actively deforming Eel River Margin, Northern California. Mar. Geol. 303, 99–114.

Jin, J.H., Chough, S.K., 1998. Partitioning of transgressive deposits in the southeastern Yellow Sea: a sequence stratigraphic interpretation. Mar. Geol. 149, 79–92.

Kennedy, M.P., 2001. Geologic map of the Las Pulgas Canyon 7.5-minute quadrangle, San Diego County, California: a digital database. California Geological Survey, Preliminary Geologic Maps, scale 1:24,000.

Kennedy, M.P., Tan, S.S., 2005. Geologic map of the Oceanside 30′ × 60′ Quadrangle. California: Regional Geologic Map Series, 1:100,000.

Kern, J.P., Rockwell, T.K., 1992. Chronology and deformation of Quaternary marine shorelines, San Diego County, California. In: Heath, E., Lewis, L. (Eds.), The Regressive Pleistocene Shoreline in Southern California: Santa Ana. California: South Coast Geological Society Annual Field Trip Guidebook 20, pp. 1–7.

Lantzsch, H., Hanebuth, T.J., Bender, V.B., Krastel, S., 2009. Sedimentary architecture of a low-accumulation shelf since the Late Pleistocene (NW Iberia). Mar. Geol. 259, 47–58.

Le Dantec, N., Hogarth, L.J., Driscoll, N.W., Babcock, J.M., Barnhardt, W.A., Schwab, W.C., 2010. Tectonic controls on nearshore sediment accumulation and submarine canyon morphology offshore La Jolla, southern California. Mar. Geol. 268, 115–128.

Legg, M.R., 1991. Developments in understanding the tectonic evolution of the California Borderlands. In: Osbourne, R.H. (Ed.)Society of Economic Paleontologists and Mineralogists Special Publication 46, pp. 291–312.

Lindvall, S., Rockwell, T.K., 1995. Holocene activity of the Rose Canyon fault, San Diego, California. J. Geophys. Res. 100 (B12), 24121–24132.

Lisiecki, L.E., Raymo, M.E., 2005. A Pliocene–Pleistocene stack of 57 globally distributed benthic $\delta^{18}O$ records. Paleoceanography 20. http://dx.doi.org/10.1029/2004PA001071.

Magistrale, H., 1993. Seismicity of the Rose Canyon fault zone near San Diego, California. Bull. Seismol. Soc. Am. 83 (6), 1971–1978.

McNey, J.L., 1979. General geology, San Onofre area. In: Fife, D.L. (Ed.), Geologic Guide of San Onofre Nuclear Generating Station and Adjacent Regions of Southern California.

Meade, B.J., Hagar, B.H., 2005. Block models of crustal motion in Southern California constrained by GPS measurements. J. Geophys. Res. 110 (B03403).

Miller, K.G., Mountain, G.S., Browning, J.V., Kominz, M., Sugarman, P.J., Christie-Blick, N., Wright, J.D., 1998. Cenozoic global sea level, sequences, and the New Jersey transect: results from coastal plain and continental slope drilling. Rev. Geophys. 36, 569–601.

Milliman, J.D., Jiezao, Z., Anchun, L., Ewing, J.I., 1990. Late Quaternary sedimentation on the outer and middle New Jersey continental shelf: results of to local deglaciation. J. Geol. 98, 966–976.

Muhs, D.R., Kennedy, G.L., Rockwell, T.K., 1994. Uranium-series ages of marine terrace corals from the Pacific coast of North America and implications for last-interglacial sea level history. Quat. Res. 42 (1), 72–87.

Nicholson, C., Sorlien, C.C., Atwater, T., Crowell, J.C., Luyendyk, B.P., 1994. Microplate capture, rotation of the western Transverse Ranges, and initiation of the San Andreas transform as a low-angle fault system. Geology 22 (6), 491–495.

Nordfjord, S., Goff, J.A., Austin, J.A., Duncan, L.S., 2009. Shallow stratigraphy and complex transgressive ravinement on the New Jersey middle and outer continental shelf. Mar. Geol. 266, 232–243.

Peltier, W.R., Fairbanks, R.G., 2006. Global glacial ice volume and last glacial maximum duration from an extended Barbados sea level record. Quat. Sci. Rev. 25, 3322–3337.

Petit, J.R., Jouzel, J., Raynaud, D., Barkov, N.I., Barnola, J.M., Basile, I., Stievenard, M., 1999. Climate and atmospheric history of the past 420,000 years from the Vostok ice core, Antarctica. Nature 399 (6735), 429–436.

Posamentier, H.W., 2002. Ancient shelf ridges — a potentially significant component of the transgressive system tract: case study from offshore northwest Java. AAPG Bull. 86, 75–106.

Posamentier, H.W., Allen, G.P., 1993. Variability of the sequence stratigraphic model: effects of local basin factors. Sediment. Geol. 86, 91–109.

Rampino, M.R., Sanders, J.E., 1981. Evolution of the barrier islands of southern Long Island, New York. Sedimentology 28, 37–47.

Rentz, P.T., 2010. The Influence of Tectonics, Sea Level, and Sediment Supply on Coastal Morphology in the Oceanside Littoral Cell, CA (UCSD Master's Thesis) .

Rockwell, T., 2010. The Rose Canyon fault zone in San Diego. Fifth International Conference on Recent Advances in Geotechnical Earthquake Engineering and Soil Dynamics.

Ryan, H.F., Legg, M.R., Conrad, J.E., Sliter, R.W., 2009. Recent faulting in the Gulf of Santa Catalina; San Diego to Dana Point. Spec. Pap. Geol. Soc. Am. 454, 291–315.

Ryan, H.F., Conrad, J.E., Paull, C.K., McGann, M., 2012. Slip rate on the San Diego Trough fault zone, inner California borderland, and the 1986 Oceanside earthquake swarm revisited. Bull. Seismol. Soc. Am. 102 (6), 2300–2312. http://dx.doi.org/10.1785/0120110317.

Schwab, W.C., Baldwin, W.E., Denny, J.F., Hapke, C.J., Gayes, P.T., List, J.H., Warner, J.C., 2014. Modification of the Quaternary stratigraphic framework of the inner-continental shelf by Holocene marine transgression: an example offshore of Fire Island, New York. Mar. Geol. 355, 346–360.

Shackleton, N.J., 2000. The 100,000-year ice-age cycle identified and found to lag temperature, carbon dioxide, and orbital eccentricity. Science 289, 1897–1902.

Shlemon, R.J., 1992. The Cristianitos fault and quaternary geology, San Onofre State Beach, California. The regressive Pleistocene shoreline in southern California. South Coast Geological Society Annual Field Trip Guidebook 20 pp. 9–12.

Sliter, Ray W., Ryan, Holly F., Triezenberg, Peter J., 2010. High-resolution seismic-reflection data offshore of Dana Point, southern California borderland. U.S. Geological Survey Open-file Report 2010-1111 (http://pubs.usgs.gov/of/2010/1111/).

Snedden, J.W., Dalrymple, R.W., 1999. Modern shelf sand ridges: from historical perspective to a unified hydrodynamic and evolutionary model. In: Bergman, K.M., Snedden, J.W. (Eds.), Isolated Shallow Marine Sand Bodies: Sequence Stratigraphic Analysis and Sedimentological Interpretation. SEPM Special Publication vol. 64, pp. 13–28.

Sorenson, J., Young, A., Driscoll, N., 2009. Tectonic Controls on Sea Cliff Geology of San Onofre State Beach. Unpublished UCSD Senior Thesis.

Swift, D.J.P., 1968. Coastal erosion and transgressive stratigraphy. J. Geol. 76, 444–456.

Swift, D.J.P., Phillips, S., Thorne, J.A., 1991. Sedimentation on continental margins: V. Parasequences. In: Swift, D.J.P., Oertel, G.F., Tillman, R.W., Thorne, J.A. (Eds.), Shelf Sand and Sandstone Bodies—Geometry, Facies and Sequence Stratigraphy. International Association of Sedimentologists Special Publication vol. 14, pp. 153–187.

Vail, P.R., Mitchum Jr., R.M., Todd, R.G., Widmier, J.M., Thompson III, S., Sangree, J.B., Bubb, J.N., Hatlelid, W.G., 1977. Seismic stratigraphy and global changes of sea-level. In: Payton, C.E. (Ed.), Seismic Stratigraphy—Applications to Hydrocarbon Exploration. American Association of Petroleum Geologists Memoir vol. 26, pp. 49–212.

Van Wagoner, J.C., Mitchum, R.M., Campion, K.M., Rahmanian, V.D., 1990. Siliciclastic sequence stratigraphy in well logs, cores, and outcrops. Am. Assoc. Pet. Geol. Methods Explor. Ser. 7 (55 pp.).